



Rox8 promotes microRNA-dependent *yki* messenger RNA decay

Xiaowei Guo^{a,1}, Yihao Sun^{a,b,1}, Taha Azad^c, H. J. Janse van Rensburg^c, Jingjing Luo^a, Shuai Yang^{d,e}, Peng Liu^{d,e}, Zhongwei Lv^a, Meixiao Zhan^b, Ligong Lu^b, Yingqun Zhou^a, Xianjue Ma^{d,e,2}, Xiaoping Zhang^{a,2}, Xiaolong Yang^{c,2}, and Lei Xue^{a,b,2}

^aInstitute of Intervention Vessel, Shanghai 10th People's Hospital, Shanghai Key Laboratory of Signaling and Diseases Research, School of Life Science and Technology, Tongji University, Shanghai 200092, China; ^bZhuhai Interventional Medical Center, Zhuhai Precision Medical Center, Zhuhai People's Hospital, Zhuhai Hospital Affiliated with Jinan University, Zhuhai, Guangdong 51900, China; ^cDepartment of Pathology and Molecular Medicine, Queen's University, Kingston, K7L 3N6, ON, Canada; ^dKey Laboratory of Growth Regulation and Translational Research of Zhejiang Province, School of Life Sciences, Westlake University, Hangzhou, Zhejiang 310024, China; and ^eInstitute of Biology, Westlake Institute for Advanced Study, Hangzhou, Zhejiang 310024, China

Edited by Norbert Perrimon, Harvard Medical School, Boston, MA, and approved September 10, 2020 (received for review June 30, 2020)

The Hippo pathway is an evolutionarily conserved regulator of organ growth and tumorigenesis. In *Drosophila*, oncogenic Ras^{V12} cooperates with loss-of-cell polarity to promote Hippo pathway-dependent tumor growth. To identify additional factors that modulate this signaling, we performed a genetic screen utilizing the *Drosophila* Ras^{V12}/*lgl*^{-/-} in vivo tumor model and identified Rox8, a RNA-binding protein (RBP), as a positive regulator of the Hippo pathway. We found that Rox8 overexpression suppresses whereas Rox8 depletion potentiates Hippo-dependent tissue overgrowth, accompanied by altered Yki protein level and target gene expression. Mechanistically, Rox8 directly binds to a target site located in the *yki* 3' UTR, recruits and stabilizes the targeting of miR-8-loaded RISC, which accelerates the decay of *yki* messenger RNA (mRNA). Moreover, TIAR, the human ortholog of Rox8, is able to promote the degradation of *yki* mRNA when introduced into *Drosophila* and destabilizes YAP mRNA in human cells. Thus, our study provides in vivo evidence that the Hippo pathway is posttranscriptionally regulated by the collaborative action of RBP and microRNA (miRNA), which may provide an approach for modulating Hippo pathway-mediated tumorigenesis.

Hippo pathway | Rox8 | TIAR | Yki | YAP

The Hippo signaling pathway, initially discovered in *Drosophila*, has emerged as an evolutionarily conserved mechanism that controls tissue growth and organ size (1–4). Deregulation of this pathway has been implicated in multiple types of human cancers (5–10). The core components of this pathway comprise a kinase cascade consisting of the kinase *Drosophila* Hippo (Hpo)/mammalian MST1/2 (11–15) that phosphorylates the downstream kinase Warts (Wts)/LATS1/2 (16, 17), which subsequently results in the phosphorylation and inactivation of the oncoprotein Yorkie (Yki)/YAP/TAZ (18, 19). When the Hippo-signaling activity is compromised, unphosphorylated Yki/YAP/TAZ translocates into the nucleus and acts as a coactivator for the transcription factor Scalloped (Sd)/TEAD1–4 to up-regulate the expression of well-described target genes involved in cell proliferation and cell death (20–22). Over the past two decades, more than 20 conserved components or regulators of this pathway have been identified, yet the mechanism by which *yki*/YAP/TAZ activity is regulated at the messenger RNA (mRNA) level remains poorly understood.

To identify modulators of the Hippo pathway, we performed a systematic genetic screen utilizing the Hippo pathway-dependent Ras^{V12}/*lgl*^{-/-} *Drosophila* tumor model (23) and identified the RNA-binding protein (RBP) Rox8 as a regulator of *yki*. RBPs play pivotal roles in posttranscriptional regulation, while dysregulated RBPs have been associated with various cancers (24–26). RBPs regulate their target genes through a wide array of mechanisms including mRNA stability, translation, and alternative splicing, underscoring the utmost importance of RBP-RNA regulatory interaction in cancers (26). We have further characterized Rox8 and

its human ortholog TIAR as a crucial regulator of mRNA stability of *Drosophila yki* and human YAP, respectively. First, overexpression of Rox8 attenuates tumor hyperplasia caused by Ras^{V12}/*lgl*^{-/-} oncogenic cooperation, while loss of Rox8 acts cooperatively with Ras^{V12} to trigger tumor overgrowth. Second, Rox8 overexpression potently diminishes whereas Rox8 depletion dramatically increases the expression of Hippo pathway-responsive target genes. In addition, Rox8 genetically functions in parallel with Yki and biochemically binds to *yki* mRNA via its 3' UTR, accelerating mRNA decay that results in decreased Yki protein level. Moreover, Rox8 executes this function by recruiting and stabilizing the targeting of miR-8-loaded RISC onto *yki* mRNA. Significantly, introduction of human TIAR into *Drosophila* executes a similar regulatory function on *yki* mRNA, Hippo pathway target genes, and tissue growth. Furthermore, TIAR destabilizes YAP mRNA via its 3' UTR in human cells and inhibits YAP-induced cell proliferation and colony formation. Thus, our study reveals that Rox8/TIAR is an evolutionarily conserved regulator of the Hippo pathway from *Drosophila* to human.

Results

Rox8 Inhibits Cell Proliferation and Tissue Growth in *Drosophila*. The oncogenic cooperation between Ras^{V12} and loss-of-cell polarity genes (*scrib*, *lgl*, *dlg*) in larval eye-antennal clones has been well-established as a *Drosophila* tumor model that includes the

Significance

Dysregulation of the evolutionarily conserved Hippo pathway has been implicated in multiple diseases including cancer. Here we identified the RNA-binding protein (RBP) Rox8 as a regulator of Hippo signaling-mediated tumorigenesis. Rox8 not only directly binds to the 3' UTR of *yki* mRNA, but also interacts with miR-8 to recruit miRNA-loaded RISC to degrade *yki* mRNA and therefore impedes Yki-induced tissue growth. We further revealed that TIAR, the human ortholog of Rox8, has retained a conserved regulatory function in *yki*/YAP mRNA stability. Our work uncovers a collaborative action of RBP and miRNA in regulating Hippo signaling.

Author contributions: X.G., Y.S., X.M., X.Z., X.Y., and L.X. designed research; X.G., Y.S., T.A., H.J.J.v.R., J.L., S.Y., and P.L. performed research; X.G., Y.S., Z.L., M.Z., L.L., Y.Z., X.M., X.Z., X.Y., and L.X. analyzed data; and X.G., Y.S., and L.X. wrote the paper.

The authors declare no competing interest.

This article is a PNAS Direct Submission.

Published under the PNAS license.

¹X.G. and Y.S. contributed equally to this work.

²To whom correspondence may be addressed. Email: lei.xue@tongji.edu.cn, maxianjue@westlake.edu.cn, zxpkyx@126.com, or yangx@queensu.ca.

This article contains supporting information online at <https://www.pnas.org/lookup/suppl/doi:10.1073/pnas.2013449117/-DCSupplemental>.

First published November 17, 2020.

massive tumor-like overgrowth and invasion into the ventral nerve cord (27). While impaired Hippo pathway is required for the overgrowth (23), JNK signaling is necessary for the invasion (9). To identify additional factors critical for tumor progression *in vivo*, we previously utilized this model to perform a genetic screen and characterized multiple regulators of JNK-mediated cell invasion (27–31). From the same screen, we found that *Ras^{V12}/lgl^{-/-}*-induced tumor overgrowth was significantly impeded by *Rox8^{EY02351}*, an *UAS*-bearing EP element inserted in the *Rox8* 5' UTR (*SI Appendix, Fig. S14*) that is able to drive *Rox8* overexpression in *Ras^{V12}/lgl^{-/-}* clones (Fig. 1 *C* and *D*), whereas the growth of control clones was not inhibited by *Rox8* overexpression (Fig. 1 *A* and *B*). As a positive control, activation of the Hippo pathway by ectopic *Wts* expression was sufficient to block *Ras^{V12}/lgl^{-/-}*-induced tumor growth (Fig. 1*E*). On the other hand, *Rox8* knockdown clones synergized with *Ras^{V12}* to promote tumorigenesis, which was confirmed by a *Rox8* null mutant generated by the CRISPR/Cas9 technique (Fig. 1 *F–I* and *SI Appendix, Figs. S1 A, B, and D and S2A*), indicating a tumor suppressor function for *Rox8*. Consistent with its tumor suppressor function, *Rox8* null mutant clones in the eye imaginal discs grow much larger than the wild-type controls (*SI Appendix, Fig. S3*). To verify the tumor suppressor function of *Rox8* in other cellular contexts, we generated *Rox8* knockdown or mutant clones in the wing imaginal discs and found that *Rox8* depletion leads to increased clonal size (Fig. 1 *K–N*). To determine whether *Rox8* plays a vital role in cell proliferation, we performed immunohistochemistry staining against PH3, a common mark for mitosis. We found that knockdown of *Rox8* in the posterior compartment of wing discs promotes cell proliferation, as indicated by ectopic PH3 incorporation (Fig. 1 *O–U* and *SI Appendix, Fig. S2B*). In addition, knockdown of *Rox8* in the midgut intestinal stem cells leads to increased clonal size and PH3 incorporation, coupled with enlarged gut width (*SI Appendix, Fig. S4 M–P*). The increased PH3 staining and gut width were confirmed in *Rox8* null mutants (*SI Appendix, Fig. S4 Q–T*), which were viable and fertile with no other discernible phenotype. To examine the gain-of-function effect of *Rox8* *in vivo*, we used *nub-Gal4* to overexpress *Rox8* (*nub > Rox8^{EY02351}*) and found that the wing size significantly decreased (*SI Appendix, Fig. S4 A–C*). *Rox8⁸⁵⁻⁵⁷²*, a GS line inserted in the first intron (*SI Appendix, Fig. S14*), appears relatively stronger than *Rox8^{EY02351}* as measured by RT-qPCR (*SI Appendix, Fig. S1C*), probably due to its proximity to the translation initiation site. Intriguingly, *ptc > Rox8⁸⁵⁻⁵⁷²* resulted in a reduced area between L3 and L4 in the wings and diminished scutellum (*SI Appendix, Fig. S4 D–I*), while *GMR > Rox8⁸⁵⁻⁵⁷²* produced a small-eye phenotype (*SI Appendix, Fig. S4 J–L*). Collectively, our findings suggest that *Rox8* curbs cell proliferation and tissue growth in development.

Rox8 Negatively Regulates Hippo Target Gene Expression. As the Hippo pathway plays an indispensable role in *Ras^{V12}/loss-of-cell-polarity*-triggered tumorigenesis (23), and overexpression of *Rox8* mimics that of *Wts* to inhibit *Ras^{V12}/lgl^{-/-}*-induced tumor growth (Fig. 1 *D* and *E*), we decided to test the genetic interaction between *Rox8* and the Hippo pathway. Intriguingly, *Ras^{V12}/Rox8-IR*-induced overgrowth was strongly suppressed in heterozygous *yki* background (Fig. 1*J*), suggesting that *Rox8* might execute its tumor suppressor function via the Hippo pathway. To verify this hypothesis, we checked the expression of three well-characterized Hippo pathway target genes: *wingless* (*wg*), *expanded* (*ex*), and *diap1* (21, 32, 33). We found that knockdown of *Rox8* notably enhanced, whereas overexpression of *Rox8* significantly diminished, the transcription of these target genes in third instar larval wing discs (Fig. 2 *A–I*). Consistently, *Diap1* and *ex-LacZ* expression were up-regulated in *Rox8* mutant clones in the wing imaginal discs (*SI Appendix, Fig. S5*). In addition, depletion of *Rox8* in midgut intestinal stem cells resulted in up-regulated *bantam*

expression, another well-described target gene of the Hippo pathway (*SI Appendix, Fig. S6*). Taken together, these data suggest that *Rox8* positively modulates the Hippo pathway.

To corroborate the genetic interaction between *Rox8* and the Hippo pathway *in vivo*, we examined the adult eye and observed a synergistic effect on eye-size enlargement between *Rox8* depletion and heterozygous *wts* mutation (*SI Appendix, Fig. S7 A–E*). Moreover, *nub > Hpo*-induced wing pouch reduction was significantly suppressed upon *Rox8* knockdown (*SI Appendix, Fig. S7 F–J*). Collectively, these data support the conclusion that *Rox8* positively regulates the Hippo pathway in development.

Rox8 Regulates the Hippo Pathway in Parallel with Yki. To unravel the mechanism by which *Rox8* regulates the Hippo pathway, we performed genetic epistasis analysis between *Rox8* and the Hippo pathway core components. Knockdown of *hpo* or *wts*, or overexpression of *Yki* along the anterior/posterior (A/P) compartment boundary by *ptc-Gal4*, dramatically enlarged the area between L3 and L4 in the adult wings (Fig. 2 *J–M*), which was significantly attenuated by mild expression of *Rox8* (*Rox8^{EY02351}*, Fig. 2 *N–R*). Consistent with previous studies that Hippo pathway regulates tissue growth by affecting cell number (18, 34, 35), we found that cell number in the area between L3 and L4 was indeed increased by *ptc > Yki*, which was significantly suppressed upon *Rox8* coexpression (Fig. 2*S*). In agreement with the adult phenotype, *ptc > Yki*-induced tissue overgrowth in the larval wing discs was potently suppressed by *Rox8* (*SI Appendix, Fig. S8 I–L*). Furthermore, mild expression of *Rox8* (*Rox8^{EY02351}*) impeded the adult-eye hyperproliferation phenotype induced by depletion of *hpo* or *wts* or overexpression of *Yki* (*SI Appendix, Fig. S8 A–H and M*). Collectively, these data suggest that *Rox8* may act genetically downstream of, or in parallel with, *yki*. However, *Ras^{V12}/Rox8-IR*-triggered tumor overgrowth and *Rox8-IR*-induced *ex-LacZ* expression were robustly attenuated by the heterozygous *yki* mutation (Fig. 1*J* and *SI Appendix, Fig. S9*), suggesting that *Rox8* may act upstream of, or in parallel with, *yki*. Collectively, our genetic epistasis data support the notion that *Rox8* regulates the Hippo pathway in parallel with *yki*.

Rox8 Impedes yki mRNA and Protein Expression. Given that *Rox8* encodes an RNA-binding protein that regulates mRNA splicing, stability, or translation (9, 26), it is plausible that *Rox8* modulates the Hippo pathway via *yki* mRNA. To test this possibility, we first checked whether *Rox8* regulates *Yki* protein expression *in vivo* and *in vitro*. In third instar larval wing discs, *Yki* protein level, as judged by immunohistochemistry staining with antibody against *Yki*, was dramatically reduced upon *Rox8* overexpression along the A/P compartment boundary driven by *ptc-Gal4* (Fig. 3*A*), but significantly increased in *Rox8* mutant clones (Fig. 3*B*). Consistently, in S2 cells, *Rox8* expression significantly diminished whereas *Rox8* knockdown increased endogenous *Yki* protein level (Fig. 3 *C* and *D*). Next, we examined if deregulated *Rox8* influences *yki* mRNA level utilizing the RT-qPCR assay. We found that *yki* mRNA decreased upon *Rox8* overexpression (Fig. 3*E*), but was elevated by *Rox8* knockdown in S2 cells (Fig. 3*F*). We further confirmed these results by RT-qPCR that *yki* mRNA was indeed negatively regulated by *Rox8* in the wing discs (Fig. 3*G*). On the other hand, *Rox8* expression did not affect *sd* mRNA level (*SI Appendix, Fig. S10*), suggesting a specific regulation of *yki* mRNA by *Rox8*. In agreement with the above data, ectopic *Rox8* suppressed the luciferase expression of 3x*Sd2-luc*, a reporter of *Yki-Sd* transcriptional activity in S2 cells (20), in a dosage-dependent manner (Fig. 3*H*). Taken together, these data indicate that *Rox8* negatively regulates *yki* expression both *in vitro* and *in vivo*.

Rox8 Promotes yki mRNA Decay via Its Binding Site in yki 3' UTR. RBPs often promote mRNA decay through direct binding to

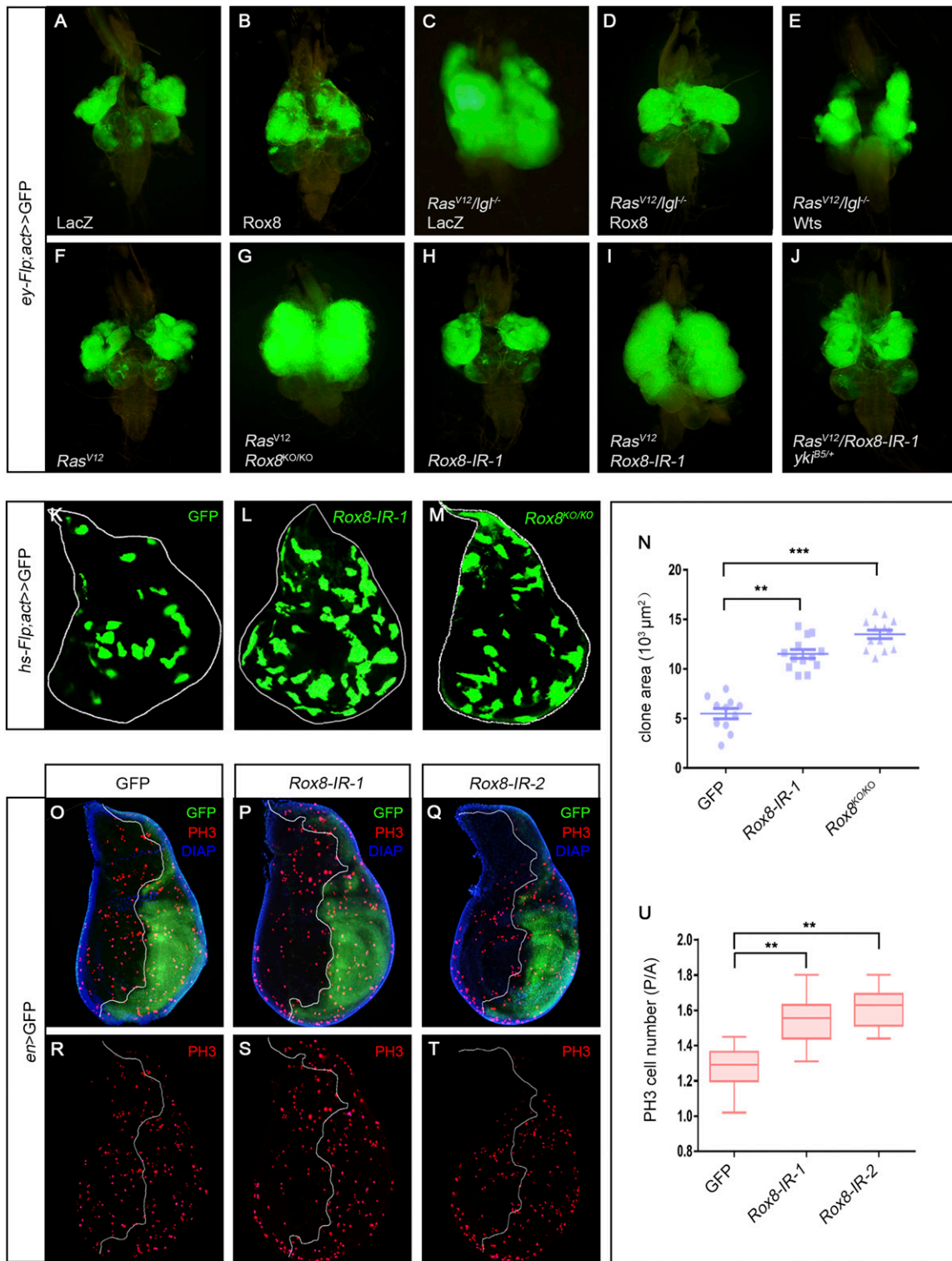


Fig. 1. Rox8 synergizes with Ras^{V12} to promote tumorigenesis. (A–J) Fluorescence micrographs of GFP-labeled clones in eye-antennal discs dissected from larvae 7 d after egg laying are shown. Compared with the control (A), *Ras^{V12}/Igf^{-/-}*-induced massive tumor overgrowth (C), which was dramatically suppressed by overexpression of Rox8 (D) or Wts (E). Meanwhile, ectopic Rox8 by itself caused no discernible phenotype (B). Ras^{V12} cooperated with Rox8 mutant (G) or RNAi (I) to trigger tumor-like overgrowth, whereas expression of Ras^{V12} (F) or Rox8.RNAi (H) alone was not sufficient to produce such a phenotype. *Ras^{V12}/Rox8-IR*-induced overgrowth was suppressed in the heterozygous *yki* mutant (J). (K–M) and (O–T) Fluorescence micrographs of third instar larval wing discs. Compared with the controls (K), *Rox8* knockdown (L) or mutant (M) clones displayed augmented clonal size. (N) Quantification of clonal size is shown in K–M. Compared with the control (O and R), *Rox8* knockdown in the posterior compartment of the wing disc led to increased PH3 staining (P, Q, S, and T). (U) Quantification of PH3-positive cell numbers in O–T. ****P* < 0.001, ***P* < 0.01.

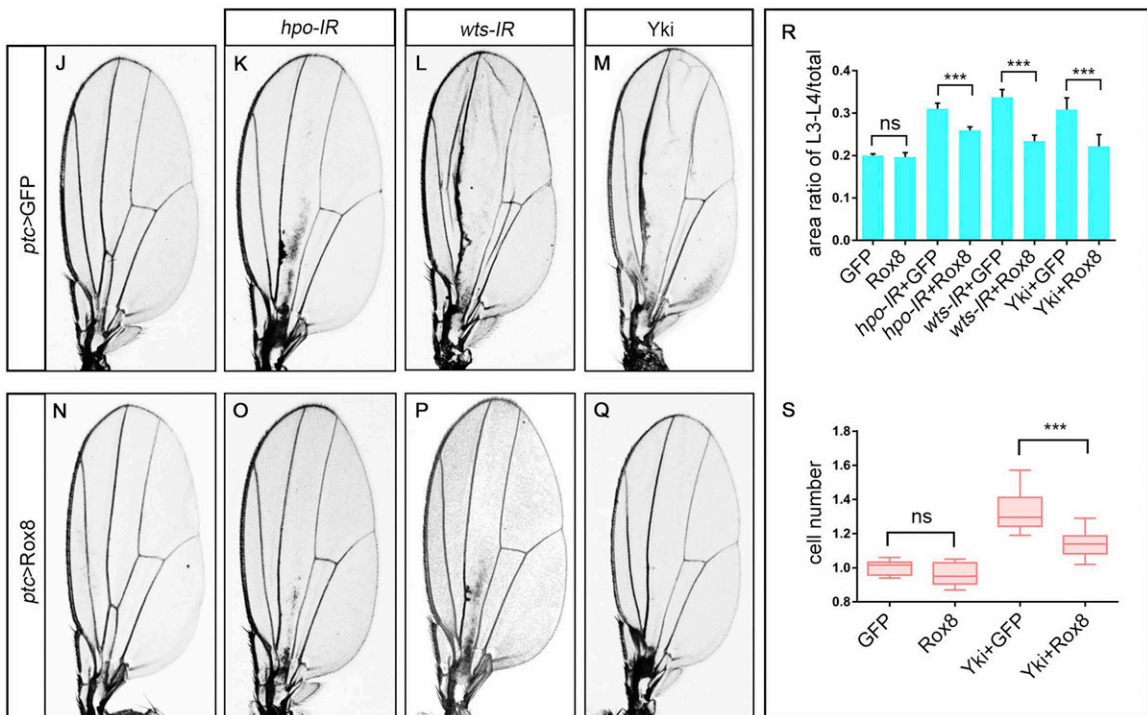
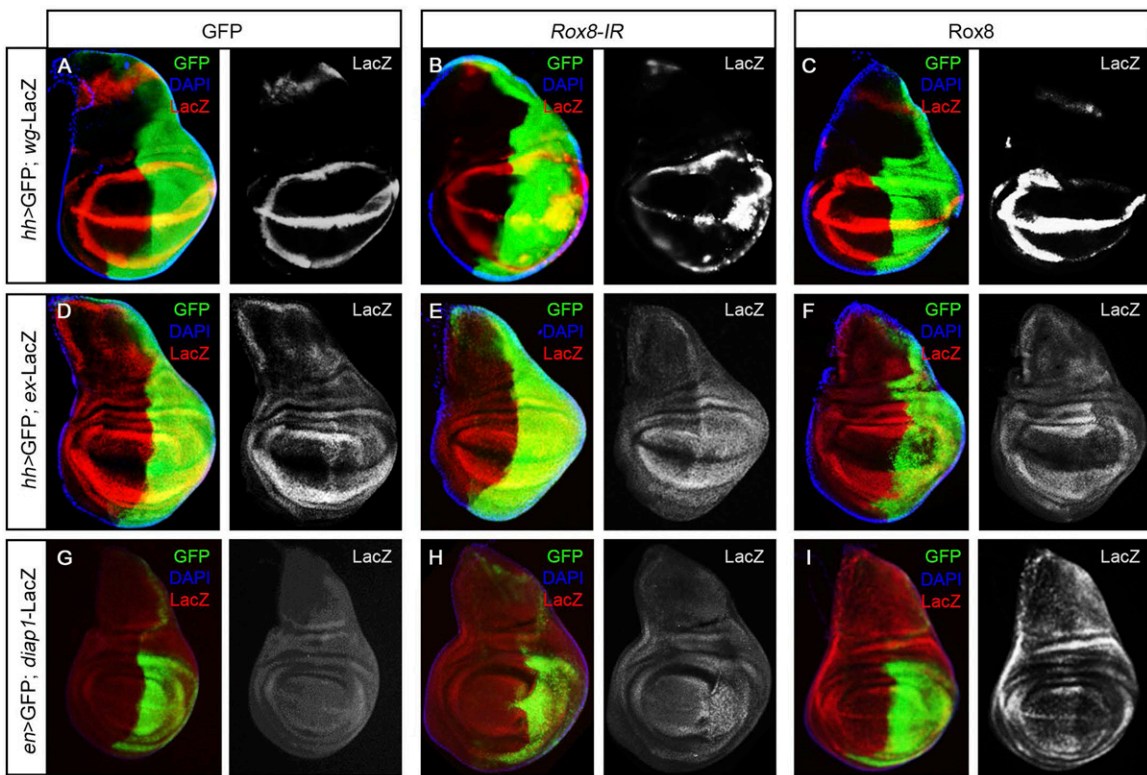


Fig. 2. Rox8 regulates Hippo pathway in development. (A–I) Fluorescence micrographs of third instar larval wing discs are shown. Compared with the control (A, D, and G), expression of *wg-LacZ* (A–C), *ex-lacZ* (D–F), or *diap1-LacZ* (G–I) was enhanced by *Rox8* depletion (B, E, and H) but impeded by *Rox8* overexpression (C, F, and I) in the posterior compartment. (J–M) and (N–Q) Light micrographs of *Drosophila* adult wings are shown. In comparison with the control (J), depletion of *hpo* (K) or *wts* (L) or overexpression of *Yki* (M) driven by *ptc-Gal4* increased the area size between L3 and L4, which were significantly suppressed by *Rox8* expression (O–Q). (R) Quantification of the area ratio of L3 to L4/total in adult wings shown in J–Q. (S) Quantification of cell number in the area between L3 and L4 shown in J, M, N, and Q. *** $P < 0.001$. ns, no significant difference. Magnification for J–Q: 4 \times .

their target sequences, usually located within the 3' UTR (26). Intriguingly, we noted two potential *Rox8*-binding sites (AUAUUUU) in the 3' UTR of *yki* mRNA (<http://cisbp-ma.ccrb.utoronto.ca/index.php>)

(Fig. 3I), raising the possibility that *Rox8* might physically interact with *yki* mRNA via these two sites. To verify whether these two sites are responsible for *Rox8*-induced *yki* mRNA decay, we

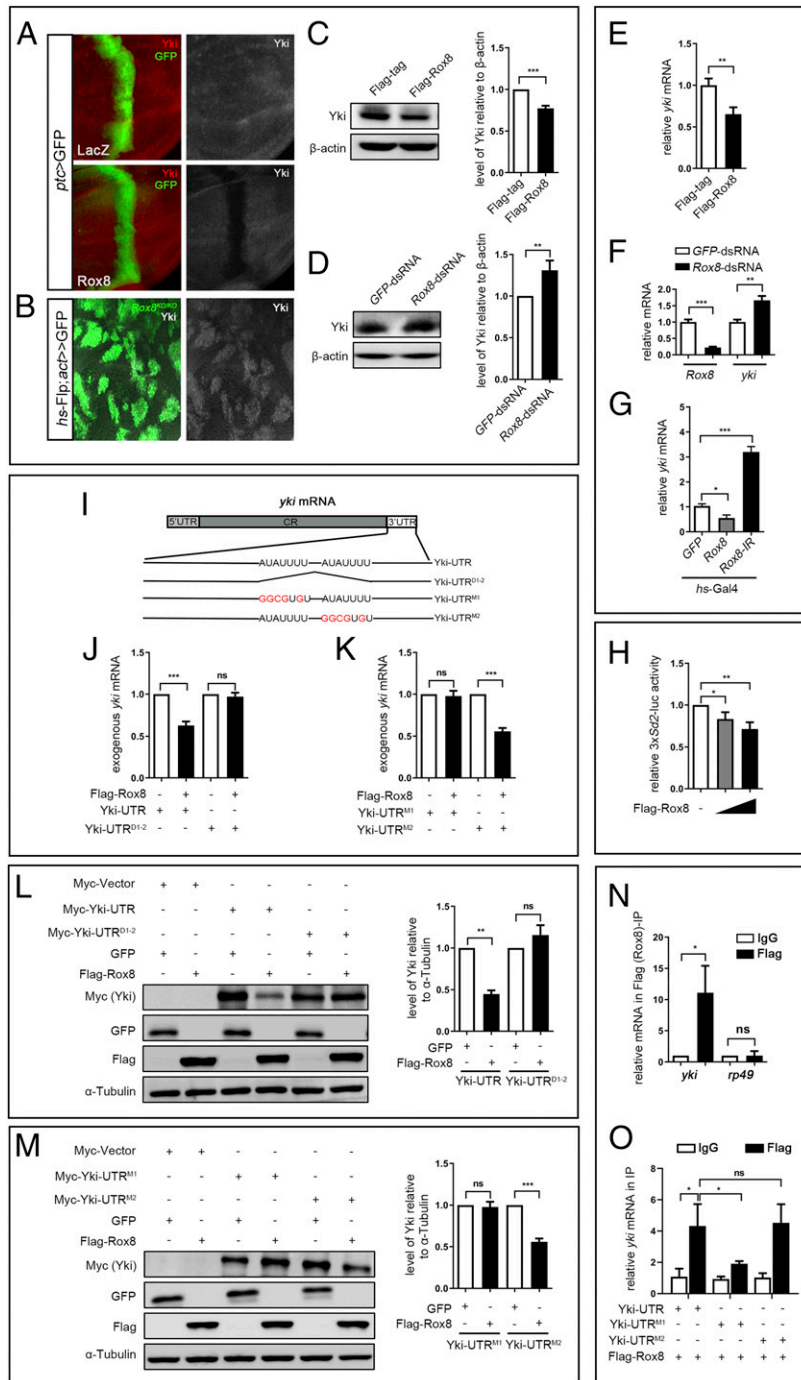


Fig. 3. Rox8 accelerates *yki* mRNA decay. (A and B) Fluorescence micrographs of wing discs are shown. Yki protein level in the wing disk was attenuated by Rox8 overexpression (A), but was up-regulated in Rox8 mutant clones (B). Yki protein level in S2 cells was decreased by Rox8 overexpression (C), but was increased by Rox8 knockdown (D). (E) *yki* mRNA level was significantly down-regulated by Rox8 overexpression in S2 cells. (F) The level of *yki* mRNA was up-regulated by knockdown of Rox8 in S2 cells. (G) RT-qPCR data showing *yki* mRNA level in larval wing discs was reduced or elevated by Rox8 overexpression or depletion driven by *hs-Gal4*. (H) The expression of 3x *Sd2-luc*, a reporter for Yki/Sd activity, was inhibited by Rox8 in a dosage-dependent manner. (I) Schematic view of *yki* mRNA with the 5' UTR, coding region (CR), and 3' UTR, which contains two potential Rox8-binding motifs (AUAUUUU). Both motifs are deleted in UTR^{D1-2}, while the first or second motif was mutated in UTR^{M1} or UTR^{M2}, respectively. (J–M) Yki-UTR, Yki-UTR^{D1-2}, Yki-UTR^{M1}, or Yki-UTR^{M2} was subcloned into pUAST-Myc-tag vector. To detect exogenous *yki* mRNA, qPCR primers were designed to span the Myc-tag and Yki coding region. Overexpressing Rox8 resulted in reduction of exogenous Yki-UTR mRNA but not Yki-UTR^{D1-2} (J). Rox8 overexpression attenuated exogenous Yki-UTR^{M2} mRNA but not Yki-UTR^{M1} (K). (L and M) Immunoblot analysis of Myc-tagged-Yki-UTR, UTR^{D1-2}, UTR^{M1}, or UTR^{M2} expression upon coexpression of Flag-Rox8 in S2 cells. (Left) Immunoblot staining. (Right) Quantification data. As shown in L, expression of Myc-Yki-UTR but not of Myc-Yki-UTR^{D1-2} was dramatically inhibited by Rox8 overexpression. (M) Expression of Myc-Yki-UTR^{M2} but not Myc-Yki-UTR^{M1} was attenuated by overexpression of Rox8. (N and O) RIP assay was performed to detect the physical interaction between Rox8 and *yki* mRNA. Rox8 specifically bound to endogenous *yki* mRNA but not to *rp49* mRNA that served as a negative control (N). The binding of Rox8 to *yki* 3' UTR was blocked by M1 mutation, but not by M2 in S2 cells (O). ****P* < 0.001, ***P* < 0.01, **P* < 0.05. ns, no significant difference.

constructed Myc-tagged Yki-UTR (with intact 3' UTR), Yki-UTR^{D1-2} (both sites are deleted from the 3' UTR), Yki-UTR^{M1} (site 1 is mutated), and Yki-UTR^{M2} (site 2 is mutated) (Fig. 3I). Cotransfection of Rox8 in S2 cells decreased the expression of Yki-UTR at both mRNA and protein levels, but had no effect on that of Yki-UTR^{D1-2} (Fig. 3J and L), suggesting that one or both sites are necessary for Rox8's activity on *yki* mRNA. Furthermore, mutation of the first site (M1), but not the second one (M2), fully

blocked Rox8-triggered *yki* mRNA and protein reduction (Fig. 3K and M), suggesting that the first site is essential for Rox8 to negatively regulate the *yki* mRNA level.

To examine the physical interaction between Rox8 and *yki* mRNA, we performed a RNA immunoprecipitation (RIP) assay. We found that endogenous *yki* mRNA, but not *rp49* mRNA, was significantly enriched by Flag-Rox8 (Fig. 3N). Consistently, ectopic Yki-UTR mRNA was also enriched by Flag-Rox8 (Fig. 3O),

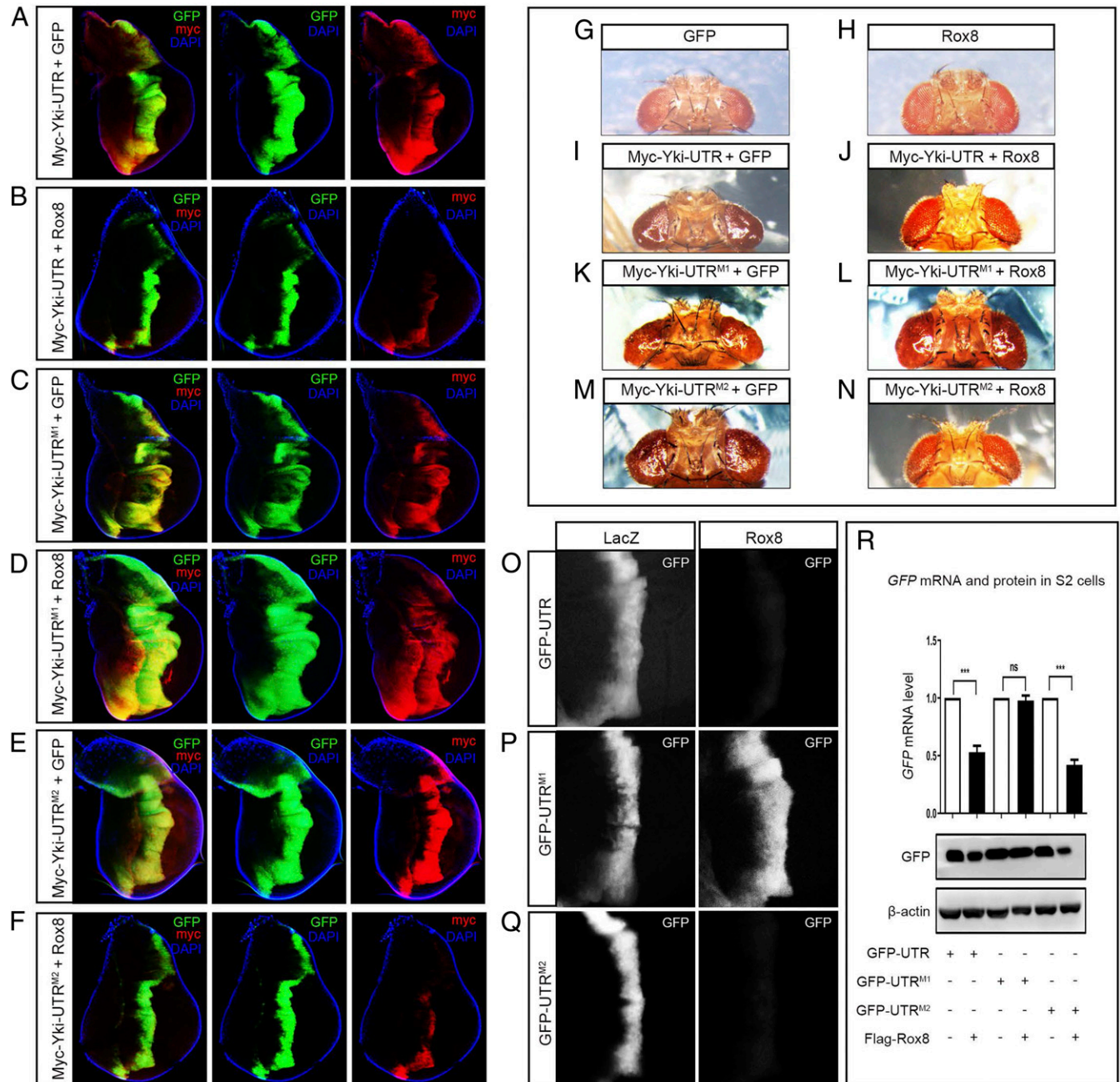


Fig. 4. The *yki* 3' UTR is necessary and sufficient for Rox8-mediated mRNA decay in vivo. (A–F) Fluorescence micrographs of wing discs are shown. Rox8 overexpression dramatically suppressed the overgrowth induced by Myc-Yki-UTR (A and B) or Myc-Yki-UTR^{M2} (E and F), but not that by Myc-Yki-UTR^{M1} (C and D). Consistently, Myc-Yki expression from Myc-Yki-UTR or Myc-Yki-UTR^{M2}, but not from Myc-Yki-UTR^{M1}, was impeded by Rox8 (A–F). (G–N) Light micrographs of *Drosophila* adult eyes are shown. Compared with the *GMR* > GFP control (G), *GMR* > Rox8 displayed no obvious phenotype (H). However, overexpression of Rox8 significantly impeded tumor-like overgrowth triggered by ectopic expression of Myc-Yki-UTR (I and J) or Myc-Yki-UTR^{M2} (M and N), but not of Myc-Yki-UTR^{M1} (K and L). (O–Q) Fluorescent images of third instar larval wing discs. Expressing Rox8 strikingly attenuated the expression of GFP from GFP-UTR (O) or GFP-UTR^{M2} (Q), but not that from GFP-UTR^{M1} (P). (R) RT-qPCR and immunoblot assays were performed in cultured S2 cells. Rox8 overexpression decreased the expression of GFP-UTR and GFP-UTR^{M2} at both the mRNA and protein level, but had no significant effect on that of GFP-UTR^{M1}. ****P* < 0.001. ns, no significant difference. Magnification for I–N: 6.3×.

and this enrichment was significantly abrogated by M1, but not by M2 (Fig. 3O), suggesting that Rox8 physically interacts with *yki* mRNA, most probably by direct binding to the first AUAUUUU motif located in the 3' UTR of *yki* mRNA.

Rox8 Requires Its Binding Site to Suppress *yki*-Induced Overgrowth. To corroborate the role of the Rox8-binding site in vivo, we generated transgenic flies expressing Myc-tagged Yki-UTR, Yki-UTR^{M1}, or Yki-UTR^{M2}. In agreement with the in vitro results, Rox8 overexpression in the wing discs driven by *ptc*-Gal4 dramatically inhibited the hyperplastic overgrowth induced by Myc-Yki-UTR or Myc-Yki-UTR^{M2}, but not that by Myc-Yki-UTR^{M1} (Fig. 4 A–F). In line with the growth phenotype, ectopic Rox8 was able to reduce Myc-Yki protein produced by Myc-Yki-UTR or Myc-Yki-UTR^{M2}, but not that by Myc-Yki-UTR^{M1} (Fig. 4 A–F). Furthermore, ectopic Rox8 suppressed adult eye overgrowth induced by Myc-Yki-UTR or Myc-Yki-UTR^{M2}, but not by Myc-Yki-UTR^{M1} (Fig. 4 G–N), confirming that the first Rox8-binding site in *yki* 3' UTR is necessary for Rox8 to impede Yki expression and Yki-induced tissue growth in vivo.

***Yki* 3' UTR Is Sufficient for Rox8-Mediated mRNA Degradation.** The above results demonstrate that the 3' UTR is necessary for *yki* mRNA to be regulated by Rox8. However, RBPs could regulate mRNA level by multiple means, including transcription, splicing, and stability. To investigate whether Rox8 regulates *yki* mRNA by affecting its stability, and whether *yki* 3' UTR is sufficient for this activity of Rox8, we made UAS– transgenes in which the 3' UTR, UTR^{M1}, or UTR^{M2} was placed after the GFP-coding region, respectively. In this setting, the transcription of *GFP* is solely controlled by the Gal4/UAS binary system, and no splicing event is involved in the production of *GFP* mRNA; hence, any effect of Rox8 on *GFP* mRNA should be achieved via influencing mRNA stability. Intriguingly, we found that both *GFP* mRNA and protein expression of GFP-UTR or GFP-UTR^{M2}, but not that of GFP-UTR^{M1}, was significantly suppressed by Rox8 in cultured S2 cells (Fig. 4R). These results were confirmed in vivo, where GFP and Rox8 were coexpressed along the A/P compartment boundary by *ptc*-Gal4 (Fig. 4 O–Q) or in the dorsal compartment by *ap*-Gal4 in the wing imaginal discs (SI Appendix, Fig. S11). Thus, *yki* 3' UTR, which carries a Rox8-binding motif, is both necessary and sufficient for Rox8-mediated mRNA degradation.

Rox8 Promotes *yki* mRNA Degradation via miR-8. To reveal the molecular mechanism by which Rox8 facilitates *yki* mRNA decay, we hypothesized that other factors affecting the stability of *yki* mRNA might be involved. The microRNA miR-8 has been previously reported to regulate *yki* mRNA stability (36, 37). Consistently, PremiR-8 overexpression has resulted in reduced *yki* mRNA and protein levels (SI Appendix, Fig. S12A and Fig. 5A), which was confirmed by miR-8 mimics (SI Appendix, Fig. S12C). Consistently, overexpression of miR-8 in the wing discs driven by *dpp*-Gal4 inhibited the expression of *ban*-LacZ (SI Appendix, Fig. S12B), an in vivo reporter of Yki activity. To test whether miR-8 is involved in Rox8-mediated *yki* degradation, we expressed Rox8 in miR-8 null mutant and found that Rox8-mediated Yki reduction was dramatically inhibited by loss of miR-8 (Fig. 5B). Consistently, the inhibitory effect of Rox8 on Yki-induced enlarged eye size was potentially cancelled by miR-8 depletion (Fig. 5C). These data suggest that miR-8 is required for Rox8-mediated *yki* mRNA degradation. Consistently, RIP analysis showed that Rox8 specifically interacted with miR-8-3p, but not with other miRNAs (Fig. 5D) predicated to target *yki* 3' UTR via the miRanda target prediction algorithm. Furthermore, Rox8 overexpression enhanced, whereas Rox8 depletion suppressed, the binding between *yki* mRNA and the miR-8/RISC complex (Fig. 5 E–G). Together, these results suggest that Rox8

promotes *yki* mRNA decay by recruiting and/or stabilizing the targeting of miR-8-loaded RISC to *yki* mRNA (Fig. 5H).

Rox8 Function in the Hippo Pathway Is Retained by Its Human Ortholog TIAR. As the Hippo pathway is evolutionarily conserved from fly to human, we next asked whether TIAR, the human ortholog of Rox8, plays a similar role in the Hippo pathway. To this end, we created UAS-TIAR transgenic flies and checked whether ectopic TIAR could regulate the Hippo pathway in *Drosophila*. We found that TIAR expression driven by *ptc*-Gal4 in the wing discs potentially reduced Yki protein (Fig. 6A). Consistently, TIAR expression driven by *hh*-Gal4 in the posterior compartment of wing discs significantly reduced the expression of Hippo target genes, as judged by the staining of *ex*-LacZ and *wg*-LacZ (Fig. 6 B–E). Additionally, we found that the *ptc* > Yki-UTR-induced wing phenotype was suppressed by a mild expression of TIAR from a weak UAS-TIAR transgene, which by itself exhibited no obvious phenotype (SI Appendix, Fig. S13 A–E). Interestingly, the fact that TIAR could also suppress the expression of GFP-UTR both in vivo (Fig. 6F) and in vitro (Fig. 6G) suggests that it is able to bind the Rox8 target site in 3' UTR and promote the degradation of mRNA. Together, these data demonstrate that TIAR could functionally substitute for Rox8 to disrupt *yki* mRNA stability in *Drosophila*.

TIAR Regulates YAP Expression in Human Cells. To examine whether TIAR regulates *YAP* mRNA in human cells, we transiently transfected TIAR into HEK293T cells and found that excessive TIAR led to decreased *YAP* expression at both the mRNA and protein levels (Fig. 6 H and I). As *YAP* encodes a bona fide oncogene implicated in a wide spectrum of human cancers (6), we investigated the interaction between TIAR and *YAP* in cancer cells. Lentiviral infection of lung cancer A549 cells with TIAR resulted in reduced *YAP* mRNA and protein (Fig. 6 J and K), accompanied by decreased cell proliferation (SI Appendix, Fig. S13F). Moreover, RIP analysis showed that TIAR specifically bound to *YAP* mRNA, but not to *GAPDH* mRNA, served as a negative control (Fig. 6L). Consistent with our finding that Rox8 promotes *yki* mRNA decay via its 3' UTR in *Drosophila*, *YAP* 3' UTR is also necessary for *YAP* mRNA degradation by TIAR, as measured by dual luciferase assay in A549 cells (Fig. 6M). Furthermore, we carried out an immunoblot assay in cultured A549 cells and found that TIAR overexpression attenuated the expression of *YAP* from complementary DNA (cDNA) with the 3' UTR (HA-*YAP*-3' UTR), but not from cDNA without it (HA-*YAP*) (Fig. 6N). Finally, we checked whether TIAR could attenuate *YAP* activity in A549 cells and found that TIAR overexpression significantly suppressed the expression of TEAD4-luciferase (Fig. 6O), a mammalian Hippo pathway reporter (38, 39), and inhibited *YAP*-UTR (with 3' UTR) but not *YAP* (without 3' UTR)-induced cell proliferation, as measured by colony formation assay (Fig. 6P). Hence, we conclude that Rox8/TIAR modulate the Hippo pathway through the regulation of *yki*/*YAP* mRNA stability in a conserved manner from *Drosophila* to human cells.

Discussion

The Hippo pathway was initially identified in *Drosophila* and was subsequently proved to be highly conserved in mammals. Numerous studies have demonstrated that dysfunction of the Hippo pathway is closely associated with various cancers (5, 40–42). For the past two decades, multiple types of regulators of this pathway have been successfully identified, most of which are posttranscriptional-modification enzymes including kinases (43–48), E3 ubiquitin ligases (33, 49–51), methyltransferases (52), and deubiquitinating enzymes (53, 54). In the current study, we performed a genetic screen in *Drosophila* using a *Ras*^{V12}/*lgt*^{−/−} triggered, Hippo pathway-dependent tumor overgrowth model and identified the RNA-binding protein

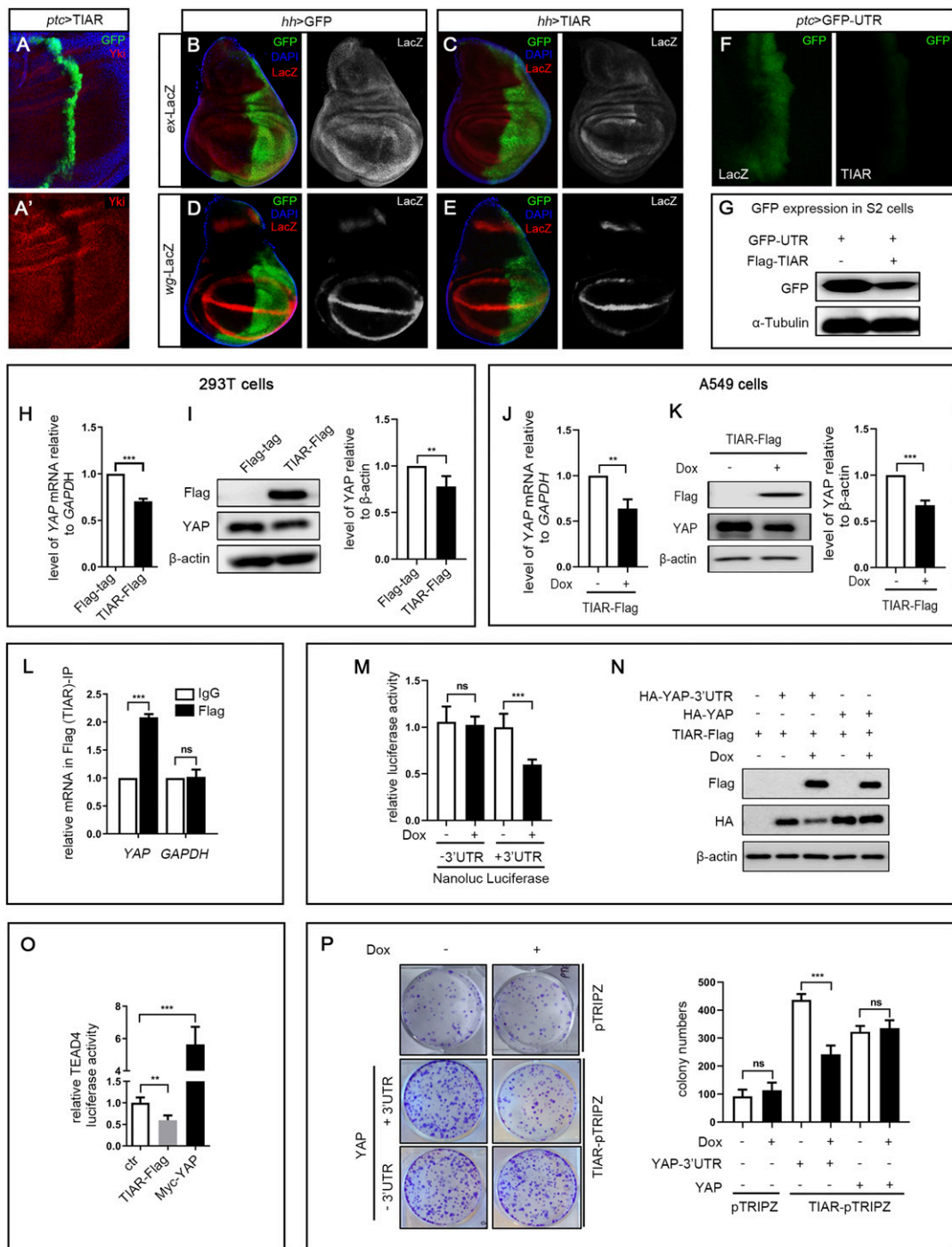


Fig. 6. Human TIAR has retained Rox8's activity on the Hippo pathway in *Drosophila* and human cells. (A–F) Fluorescent images of third instar larval wing discs. (A) *ptc* > TIAR resulted in down-regulation of Yki protein. Compared with the control (B and D), ectopic TIAR driven by *hh*-Gal4 led to reduced expression of *ex-lacZ* (C) and *wg-LacZ* (E). (F) *ptc* > TIAR dramatically suppressed the expression of GFP-UTR. (G) In cultured S2 cells, TIAR overexpression decreased GFP-UTR expression. Overexpression of TIAR transiently transfected into 293T cells inhibited YAP mRNA (H) and protein (I) expression. (Right) Quantification data of immunoblot analysis. (J–K) Overexpression of TIAR decreased YAP mRNA (J) and protein (K) level in A549 cells. A549-TIAR-Flag was untreated (–Dox) or treated (+Dox) for 2 d, followed by RT-qPCR and immunoblot assay. (Right) Quantification of immunoblot analysis. (L) Compared with IgG, YAP mRNA was significantly enriched in Flag (TIAR) immunoprecipitates, whereas *GAPDH* mRNA remained unchanged. (M) Nanoluciferase reporter assay. pMir-Nanoluc vector (–3' UTR) or pMir-Nanoluc with YAP 3' UTR (+3' UTR) was cotransfected with pGL3-control plasmid into TIAR-Flag-pTRIPZ cells. Cells were cultured in the absence (–Dox) or presence (+Dox) of Dox for 2 d, followed by luciferase assays. The ratio of relative luciferase activity for +Dox/–Dox is shown as fold changes. (N) TIAR suppressed YAP stability in A549 cells through 3' UTR region. Plasmid expressing HA-YAP with or without 3' UTR was cotransfected with TIAR-Flag plasmid into A549 cells, followed by no treatment or treatment with Dox for 2 d. Western blot was used to examine the levels of YAP-HA in cells. (O) TIAR overexpression inhibited the TEAD4-luc activity, and Myc-YAP as a positive control up-regulated the luciferase activity. (P) TIAR suppressed YAP-induced increased colony formation. Dox-inducible pTRIPZ vector or TIAR-pTRIPZ was cotransfected with plasmid expressing YAP with or without 3' UTR. The transfected cells were selected in puromycin. About 1,000 cells were plated into each well of a six-well plate, followed by no treatment or treatment with Dox. Nine days later, the colonies were fixed and stained with crystal violet. (Right) Quantification data of colony formation assays. ****P* < 0.001, ***P* < 0.01. ns, no significant difference.

RBPs have been reported to regulate transcription, mRNA processing, and translation, yet the role of RBPs in the Hippo pathway has remained largely elusive. A recent study found that *Drosophila* RBP Hrb27C regulates Yki phosphorylation indirectly via an unknown mechanism (55). In addition, two RBPs, Dnd1 and FUS, were shown to stabilize LATS mRNA in cultured hepatocellular carcinoma cells (56, 57). Yet, our findings provide in vivo and physiological evidence that an RBP directly regulates the Hippo pathway and that this regulatory mechanism has been evolutionarily conserved from fly to human.

Recent studies suggest that RBPs can either cooperate or compete with microRNAs to regulate target gene expression (58–60). In *Drosophila*, removal of a potential miR-8 seed sequence in *yki* mRNA 3' UTR leads to *yki* mRNA accumulation (36). Therefore, it would be intriguing to determine whether Rox8 acts in concert with miR-8 to modulate *yki* mRNA stability. In this study, we found that miR-8 is required for Rox8 to modulate *yki* expression and that Rox8 mechanistically promotes the decay of *yki* mRNA through facilitating the targeting of miR-8–loaded RISC into *yki* mRNA. Since our previous study showed that Yki negatively regulates Rox8 expression via bantam (9), it appears that there exists an exquisite regulatory circuit between Yki and Rox8 (Fig. 5H), which might fine-tune tissue homeostasis in development and ensure that Yki activity is turned off when Hippo signaling is active.

While the current study suggests that Rox8 acts as a tumor suppressor, Rox8 null mutants are viable and fertile with no discernible phenotype, implying that Rox8 is dispensable for normal development, which has been reported for other tumor suppressors, such as P53. However, loss of Rox8 synergizes with Ras^{V12} to induce yki-dependent tumorigenesis. Consistently, it is convincingly accepted that oncogenic cooperation between Ras^{V12} and loss of tumor suppressor genes triggers tumor growth and progression (23, 61–63). In addition, a previous study has demonstrated that the Hippo pathway interacts with Ras signaling to synergistically promote hyperproliferation and tumor development (64). These results indicate that Rox8 mutants are more prone to tumor formation and that the regulatory mechanism of Rox8–Yki may be more important under stressful conditions or in diseases. Given that mutated or deregulated RAS family genes (*HRAS*, *NRAS*, and *KRAS*) are frequently associated with various cancers (65, 66), our data suggest that TIAR may be a potential therapeutic target for not only the Hippo pathway but also for RAS-relevant cancer treatment.

Materials and Methods

Drosophila Stocks and Genetics. Flies were raised on standard *Drosophila* media, and crosses were performed at 25 °C unless otherwise indicated. For

experiments involving *tub-Gal80^{ts}*, larvae were raised at 18 °C to restrict Gal4 activity for 7 d and shifted to 29 °C for 2 d. The following fly stocks have been described previously (9, 27): *w¹¹¹⁸*, *GMR-Gal4*, *ptc-Gal4*, *ap-Gal4*, *dpp-Gal4*, *UAS-Ras^{V12}*, *Igf⁴*, *UAS-GFP*, and *UAS-Dcr*. Strains obtained from the Bloomington *Drosophila* Stock Center are *UAS-LacZ* (#3956), *Rox8^{EF02351}* (#15865), *UAS-Wts* (#30099), *UAS-Hpo* (#27105), *UAS-mir-8* (#41176), *mir-8^{d2}* (#58932), and *mir-8-sp* (#61374). Strains received from the Vienna *Drosophila* RNAi Center are *UAS-Rox8-RNAi* (#41439, referred as *UAS-Rox8-IR-1*), *UAS-wts-RNAi* (#106174), and *UAS-hpo-RNAi* (#104169). *UAS-Rox8* (G517980) and *UAS-Rox8* (*s-572*) were acquired from the Kyoto Stock Center. *UAS-Rox8-RNAi* (#5422R-1, referred as *UAS-Rox8-IR-2*) was obtained from the National Institute of Genetics. *Rox8^{KO}* mutation was generated by a germline-specific Cas9/single-guide RNA system. Fluorescently labeled invasive tumors were produced by the following strains: *y w, ey-Flp; tub-Gal80, FRT40A; act>y+>Gal4, UAS-GFP* (40A tester), *Igf⁴ FRT40A UAS-Ras^{V12}*, and *ey-Flp, act > y+>Gal4, UAS-GFP. UAS-yki, ex-lacZ, ban-LacZ, and Diap1-lacZ* were gifts from Lei Zhang, Shanghai Institute of Biochemistry and Cell Biology, Shanghai, China. *wts* mutant was a gift from Shian Wu, Nankai University, Tianjin, China.

Immunostaining of Discs. Immunostaining of discs was performed as previously described. In brief, third-instar larvae were dissected in phosphate-buffered saline (PBS) and fixed in freshly made 4% formaldehyde in PBS at room temperature for 20 min and then washed three times with PBST (PBS plus 0.1% Triton X-100). Larvae were incubated overnight with primary antibodies in PBST at 4 °C, then washed with PBST three times, and incubated with the corresponding fluorophore-conjugated secondary antibody for 2 h at room temperature. After being washed three times in PBST, discs were dissected and mounted in 40% glycerol. Images were captured with an Olympus stereo microscope SZX16. Antibodies used in this study were as follows: mouse anti-β-Gal (1:500) (Developmental Studies Hybridoma Bank); rabbit anti-PH3 (1:400) (Cell Signaling Technology); rabbit anti-Yki (1:1,000, a gift from Lei Zhang); and mouse anti-Myc (1:500, Santa Cruz). Secondary antibodies used in this study were purchased from Life Technologies and were diluted at 1:500.

Data Availability. All study data are included in the article and supporting information. Some study data are available upon request.

ACKNOWLEDGMENTS. We thank Bloomington *Drosophila* Stock Center; Vienna *Drosophila* RNAi Center; the Kyoto Stock Center; Fly Stocks of National Institute of Genetics; the Core Facility of *Drosophila* Resource and Technology at the Shanghai Institute of Biochemistry and Cell Biology of the Chinese Academy of Sciences; Developmental Studies Hybridoma Bank; Lei Zhang for fly stocks and antibodies; Rejie Jiao, Lei Zhang, and Fan Zhang for plasmids; and Xinyao Li for technical assistance. This work is supported by the National Natural Science Foundation of China (Grants 31771595 and 31970536) and the Shanghai Committee of Science and Technology (Grants 09D2260100, 18430711600, and 18140900400) (to L.X.); the China Postdoctoral Science Foundation (Grant 2000229071) (to X.G.); the Canadian Institute of Health Research (Grants MOP119325 and MOP148629); the Canadian Cancer Society (X.Y.); and the National Natural Science Foundation of China (Grant 81671716) (to Z.L.). X.M. is partially supported by “Team for Growth Control and Size Innovative Research” (Grant 201804016).

- L. Zhang, T. Yue, J. Jiang, Hippo signaling pathway and organ size control. *Fly (Austin)* **3**, 68–73 (2009).
- G. Halder, R. L. Johnson, Hippo signaling: Growth control and beyond. *Development* **138**, 9–22 (2011).
- D. Pan, Hippo signaling in organ size control. *Genes Dev.* **21**, 886–897 (2007).
- M. Yin, L. Zhang, Hippo signaling: A hub of growth control, tumor suppression and pluripotency maintenance. *J. Genet. Genomics* **38**, 471–481 (2011).
- F. X. Yu, B. Zhao, K. L. Guan, Hippo pathway in organ size control, tissue homeostasis, and cancer. *Cell* **163**, 811–828 (2015).
- F. Zanconato, M. Cordenonsi, S. Piccolo, YAP/TAZ at the roots of cancer. *Cancer Cell* **29**, 783–803 (2016).
- B. Zhao, L. Li, Q. Lei, K. L. Guan, The hippo-YAP pathway in organ size control and tumorigenesis: An updated version. *Genes Dev.* **24**, 862–874 (2010).
- D. Pan, The hippo signaling pathway in development and cancer. *Dev. Cell* **19**, 491–505 (2010).
- X. Ma *et al.*, Hippo signaling promotes JNK-dependent cell migration. *Proc. Natl. Acad. Sci. U.S.A.* **114**, 1934–1939 (2017).
- B. Zhao, Q. Y. Lei, K. L. Guan, The hippo-YAP pathway: New connections between regulation of organ size and cancer. *Curr. Opin. Cell Biol.* **20**, 638–646 (2008).
- S. Wu, J. Huang, J. Dong, D. Pan, Hippo encodes a Ste-20 family protein kinase that restricts cell proliferation and promotes apoptosis in conjunction with salvador and warts. *Cell* **114**, 445–456 (2003).
- R. S. Udan, M. Kango-Singh, R. Nolo, C. Tao, G. Halder, Hippo promotes proliferation arrest and apoptosis in the Salvador/Warts pathway. *Nat. Cell Biol.* **5**, 914–920 (2003).
- K. F. Harvey, C. M. Pflieger, I. K. Hariharan, The *Drosophila* Mst ortholog, hippo, restricts growth and cell proliferation and promotes apoptosis. *Cell* **114**, 457–467 (2003).
- S. Pantalacci, N. Tapon, P. Léopold, The Salvador partner Hippo promotes apoptosis and cell-cycle exit in *Drosophila*. *Nat. Cell Biol.* **5**, 921–927 (2003).
- J. Jia, W. Zhang, B. Wang, R. Trinko, J. Jiang, The *Drosophila* Ste20 family kinase dMST functions as a tumor suppressor by restricting cell proliferation and promoting apoptosis. *Genes Dev.* **17**, 2514–2519 (2003).
- R. W. Justice, O. Zilian, D. F. Woods, M. Noll, P. J. Bryant, The *Drosophila* tumor suppressor gene warts encodes a homolog of human myotonic dystrophy kinase and is required for the control of cell shape and proliferation. *Genes Dev.* **9**, 534–546 (1995).
- T. Xu, W. Wang, S. Zhang, R. A. Stewart, W. Yu, Identifying tumor suppressors in genetic mosaics: The *Drosophila* *lats* gene encodes a putative protein kinase. *Development* **121**, 1053–1063 (1995).
- J. Huang, S. Wu, J. Barrera, K. Matthews, D. Pan, The Hippo signaling pathway coordinately regulates cell proliferation and apoptosis by inactivating Yorkie, the *Drosophila* Homolog of YAP. *Cell* **122**, 421–434 (2005).
- B. Zhao *et al.*, Inactivation of YAP oncoprotein by the Hippo pathway is involved in cell contact inhibition and tissue growth control. *Genes Dev.* **21**, 2747–2761 (2007).
- L. Zhang *et al.*, The TEAD/TEF family of transcription factor Scalloped mediates Hippo signaling in organ size control. *Dev. Cell* **14**, 377–387 (2008).

21. S. Wu, Y. Liu, Y. Zheng, J. Dong, D. Pan, The TEAD/TEF family protein Scalloped mediates transcriptional output of the Hippo growth-regulatory pathway. *Dev. Cell* **14**, 388–398 (2008).
22. B. Zhao *et al.*, TEAD mediates YAP-dependent gene induction and growth control. *Genes Dev.* **22**, 1962–1971 (2008).
23. M. Atkins *et al.*, An ectopic network of transcription factors regulated by hippo signaling drives growth and invasion of a malignant tumor model. *Curr. Biol.* **26**, 2101–2113 (2016).
24. B. Kechavarzi, S. C. Janga, Dissecting the expression landscape of RNA-binding proteins in human cancers. *Genome Biol.* **15**, R14 (2014).
25. J. Wang, Q. Liu, Y. Shyr, Dysregulated transcription across diverse cancer types reveals the importance of RNA-binding protein in carcinogenesis. *BMC Genomics* **16** (suppl. 7), S5 (2015).
26. B. Pereira, M. Billaud, R. Almeida, RNA-binding proteins in cancer: Old players and new actors. *Trends Cancer* **3**, 506–528 (2017).
27. S. Zhang *et al.*, Wntless modulates activator protein-1-mediated tumor invasion. *Oncogene* **38**, 3871–3885 (2019).
28. X. Ma *et al.*, Myc suppresses tumor invasion and cell migration by inhibiting JNK signaling. *Oncogene* **36**, 3159–3167 (2017).
29. Y. Sun *et al.*, MKK3 modulates JNK-dependent cell migration and invasion. *Cell Death Dis.* **10**, 149 (2019).
30. X. Ma *et al.*, Rho1-Wnd signaling regulates loss-of-cell polarity-induced cell invasion in *Drosophila*. *Oncogene* **35**, 846–855 (2016).
31. X. Ma *et al.*, dUev1a modulates TNF-JNK mediated tumor progression and cell death in *Drosophila*. *Dev. Biol.* **380**, 211–221 (2013).
32. E. Cho *et al.*, Delineation of a Fat tumor suppressor pathway. *Nat. Genet.* **38**, 1142–1150 (2006).
33. X. Ma, X. Guo, H. E. Richardson, T. Xu, L. Xue, POSH regulates Hippo signaling through ubiquitin-mediated expanded degradation. *Proc. Natl. Acad. Sci. U.S.A.* **115**, 2150–2155 (2018).
34. H. Liu, D. Jiang, F. Chi, B. Zhao, The Hippo pathway regulates stem cell proliferation, self-renewal, and differentiation. *Protein Cell* **3**, 291–304 (2012).
35. B. V. Reddy, K. D. Irvine, Regulation of *Drosophila* glial cell proliferation by Merlin-Hippo signaling. *Development* **138**, 5201–5212 (2011).
36. T. Umegawachi *et al.*, Control of tissue size and development by a regulatory element in the *yorkie* 3'UTR. *Am. J. Cancer Res.* **7**, 673–687 (2017).
37. M. Sander, T. Eichenlaub, H. Herranz, Oncogenic cooperation between Yorkie and the conserved microRNA *miR-8* in the wing disc of *Drosophila*. *Development* **145**, dev153817 (2018).
38. S. Jiao *et al.*, A peptide mimicking VGLL4 function acts as a YAP antagonist therapy against gastric cancer. *Cancer Cell* **25**, 166–180 (2014).
39. W. Zhang *et al.*, VGLL4 functions as a new tumor suppressor in lung cancer by negatively regulating the YAP-TEAD transcriptional complex. *Cell Res.* **24**, 331–343 (2014).
40. Y. Han, Analysis of the role of the Hippo pathway in cancer. *J. Transl. Med.* **17**, 116 (2019).
41. S. Moon, S. Yeon Park, H. Woo Park, Regulation of the Hippo pathway in cancer biology. *Cell. Mol. Life Sci.* **75**, 2303–2319 (2018).
42. K. F. Harvey, X. Zhang, D. M. Thomas, The Hippo pathway and human cancer. *Nat. Rev. Cancer* **13**, 246–257 (2013).
43. H. L. Chung, G. J. Augustine, K. W. Choi, *Drosophila* Schip1 links expanded and tao-1 to regulate hippo signaling. *Dev. Cell* **36**, 511–524 (2016).
44. J. C. Boggiano, P. J. Vanderzalm, R. G. Fehon, Tao-1 phosphorylates Hippo/MST kinases to regulate the Hippo-Salvador-Warts tumor suppressor pathway. *Dev. Cell* **21**, 888–895 (2011).
45. C. L. Poon, X. Zhang, J. I. Lin, S. A. Manning, K. F. Harvey, Homeodomain-interacting protein kinase regulates Hippo pathway-dependent tissue growth. *Curr. Biol.* **22**, 1587–1594 (2012).
46. J. Chen, E. M. Verheyen, Homeodomain-interacting protein kinase regulates Yorkie activity to promote tissue growth. *Curr. Biol.* **22**, 1582–1586 (2012).
47. H. L. Huang *et al.*, Par-1 regulates tissue growth by influencing hippo phosphorylation status and hippo-salvador association. *PLoS Biol.* **11**, e1001620 (2013).
48. Y. S. Cho *et al.*, Regulation of Yki/Yap subcellular localization and Hpo signaling by a nuclear kinase PRP4K. *Nat. Commun.* **9**, 1657 (2018).
49. L. Hu *et al.*, The *Drosophila* F-box protein Slimb controls dSmurf protein turnover to regulate the Hippo pathway. *Biochem. Biophys. Res. Commun.* **482**, 317–322 (2017).
50. P. Ribeiro, M. Holder, D. Frith, A. P. Snijders, N. Tapon, Crumbs promotes expanded recognition and degradation by the SCF(Slimb/β-TrCP) ubiquitin ligase. *Proc. Natl. Acad. Sci. U.S.A.* **111**, E1980–E1989 (2014).
51. B. Ma *et al.*, Hypoxia regulates Hippo signalling through the SIAH2 ubiquitin E3 ligase. *Nat. Cell Biol.* **17**, 95–103 (2015).
52. L. Fang *et al.*, SET1A-mediated mono-methylation at K342 regulates YAP activation by blocking its nuclear export and promotes tumorigenesis. *Cancer Cell* **34**, 103–118.e9 (2018).
53. X. Sun *et al.*, Usp7 regulates Hippo pathway through deubiquitinating the transcriptional coactivator Yorkie. *Nat. Commun.* **10**, 411 (2019).
54. A. Toloczko *et al.*, Deubiquitinating enzyme USP9X suppresses tumor growth via LATS kinase and core components of the hippo pathway. *Cancer Res.* **77**, 4921–4933 (2017).
55. J. Mach *et al.*, Modulation of the Hippo pathway and organ growth by RNA processing proteins. *Proc. Natl. Acad. Sci. U.S.A.* **115**, 10684–10689 (2018).
56. W. Xu, F. Gong, T. Zhang, B. Chi, J. Wang, RNA-binding protein Dnd1 inhibits epithelial-mesenchymal transition and cancer stem cell-related traits on hepatocellular carcinoma cells. *Biotechnol. Lett.* **39**, 1359–1367 (2017).
57. L. Bao *et al.*, A FUS-LATS1/2 Axis inhibits hepatocellular carcinoma progression via activating hippo pathway. *Cell. Physiol. Biochem.* **50**, 437–451 (2018).
58. S. A. Ciafrè, S. Galardi, microRNAs and RNA-binding proteins: A complex network of interactions and reciprocal regulations in cancer. *RNA Biol.* **10**, 935–942 (2013).
59. P. Jiang, M. Singh, H. A. Collier, Computational assessment of the cooperativity between RNA binding proteins and microRNAs in transcript decay. *PLOS Comput. Biol.* **9**, e1003075 (2013).
60. M. Kedde, R. Agami, Interplay between microRNAs and RNA-binding proteins determines developmental processes. *Cell Cycle* **7**, 899–903 (2008).
61. X. Ma *et al.*, PP6 disruption synergizes with oncogenic Ras to promote JNK-dependent tumor growth and invasion. *Cell Rep.* **19**, 2657–2664 (2017).
62. M. Wu, J. Pastor-Pareja, T. Xu, Interaction between RasV12 and scribble clones induces tumour growth and invasion. *Nature* **463**, 545–548 (2010).
63. R. A. Pagliarini, T. Xu, A genetic screen in *Drosophila* for metastatic behavior. *Science* **302**, 1227–1231 (2003).
64. J. Pascual *et al.*, Hippo reprograms the transcriptional response to Ras signaling. *Dev. Cell* **42**, 667–680.e4 (2017).
65. M. B. Ryan, C. J. Der, A. Wang-Gillam, A. D. Cox, Targeting RAS-mutant cancers: Is ERK the key? *Trends Cancer* **1**, 183–198 (2015).
66. B. Vogelstein *et al.*, Cancer genome landscapes. *Science* **339**, 1546–1558 (2013).